Mon. Not. R. Astron. Soc. **000**, 1–?? (2010) Printed 29 May 2012 (MN LATEX style file v2.2)

arXiv:1205.6149v1 [astro-ph.HE] 28 May 2012

Non-variable TeV emission from the extended jet of a blazar in the stochastic acceleration scenario: the case of the hard TeV emission of 1ES 1101-232

Dahai Yan, Houdun Zeng, and Li Zhang[⋆]
Department of Physics, Yunnan University, Kunming, China

29 May 2012

ABSTRACT
The detections of X-ray emission from the kiloparsec-scale jets of blazars and radio galaxies may imply the existence of high energy electrons in these extended jets, and these electrons could produce high energy emission through inverse Compton (IC) process. In this paper we study the non-variable hard TeV emission from a blazar. The multi-band emission consists of two components: one is the traditional synchrotron self-Compton (SSC) emission from the inner jet, and the other is the emission produced via SSC and IC scattering of cosmic microwave background (CMB) photons (IC/CMB) and extragalactic background light (EBL) photons (IC/EBL) by relativistic electrons in the extended jet under the stochastic acceleration scenario. Such a model is applied to 1ES 1101-232. The results indicate that (1) the non-variable hard TeV emission of 1ES 1101-232 can be reproduced well, which is dominated by IC/CMB emission from the extended jet, using three characteristic values of Doppler factor ($\delta_{\rm D} = 5, 10, 15$) for the TeV emitting region in the extended jet; and (2) in the cases of $\delta_{\rm D} = 15$ and 10, the physical parameters can achieve the equipartition (or quasi-equipartition) between the relativistic electrons and the magnetic field; In contrast, the physical parameters largely deviate from the equipartition for the case of $\delta_{\rm D} = 5$. It is therefore concluded that the TeV emission region of 1ES 1101-232 in the extended jet should be moderately or highly beamed.

Key words: galaxies: BL Lacertae objects: individual: 1ES 1101-232 – galaxies: active – gamma-rays: general – radiation mechanisms: non-thermal

1 INTRODUCTION

Blazars are the most extreme class of active galactic nuclei (AGNs). Their spectral energy distributions (SEDs) are characterized by two distinct bumps: the first bump located at low-energy band is dominated by the synchrotron emission of relativistic electrons in a relativistic jet, and the second bump located at high-energy band could be produced by IC scattering (e.g., Böttcher 2007). Various soft photon sources seed SSC process (e.g., Rees 1967; Maraschi et al. 1992) and external Compton (EC) process (e.g., Dermer & Schlickeiser 1993; Sikora et al. 1994) in the jet to produce γ-rays. Hadronic models have also been proposed to explain the multi-band emissions of blazars (e.g., Mannheim 1993; Mücke et al. 2003).

More than 40 blazars have been detected in TeV band and most of them are high frequency-peaked BL Lac objects (HBLs). GeV - TeV photons from blazars would be absorbed by interaction with EBL photons, through the pair-production process (e.g., Stecker et al. (1992)). Therefore, the observed high energy emission from a TeV blazar must be less luminous and its spectrum must be steeper compared with its intrinsic emission. A large number of observational evidences support that the TeV emissions of HBLs can be explained by the SSC radiation inside their jets. However, the recent observations of TeV emission from some HBLs challenge the classic SSC scenario. Indeed, the intrinsic TeV spectra of some relatively distant sources (e.g. 1ES 0229+200, z = 0.14, Aharonian et al. (2007a); 1ES 1101-232, z = 0.186, Aharonian et al. (2006); 1ES 0347-121, z=0.188, Aharonian et al. (2007b)) are very hard (the intrinsic TeV spectral index $\Gamma_{\rm int} \sim 1.5$), even considering the low level EBL models (e.g., Franceschini et al. (2008); Finke et al. (2010)). The standard shock acceleration theories predict the particle distribution index $p \geqslant 2$, where $n(\gamma) = \gamma^{-p}$. This would correspond to a limiting intrinsic photon spectral index $\Gamma_{\rm int} \geqslant 1.5$. Moreover, as the suppression of the cross-section due to Klein-Nishina (KN) effect becomes im-

---

[⋆] E-mail: lizhang@ynu.edu.cn

portant in the TeV emission from HBLs, steeper intrinsic photon spectra would be expected.

Many possible solutions have been proposed to overcome this problem of hard TeV emission. Katarzyński et al. (2006a) suggested that the hard TeV emission of 1ES 1101-232 could be explained in SSC scenario by assuming a narrow high energy electrons distribution with a large value of minimum energy cutoff ($\sim 10^5$). As shown in Tavecchio et al. (2009), this solution might be supported by the simultaneous UV and X-ray observations of 1ES 0229+200 performed by the *Swift* satellite. While this scenario would require that emission process should be very inefficient but acceleration process should be very efficient. The formation of such hard TeV emission also would be achieved in an internal absorption scenario (Aharonian et al. 2008; Zacharopoulou et al. 2011). Very recently, Lefa et al. (2011a) suggested that considering either adiabatic losses or relativistic Maxwell-like distributions formed by a stochastic acceleration is an alternative option to create hard TeV spectra. Lefa et al. (2011b) shown that the relative hard γ-ray spectrum of Mkn 501 could be formed in a multi-zone model in the stochastic acceleration scenario. The secondary gamma-rays produced relatively close to the Earth by the interactions of cosmic ray protons with background photon can also explain the hard TeV emission of blazars (e.g., Essey et al. (2011)).

Previous works usually considered the emissions from the inner jets (sub-parsec scale) of blazars. Alternatively, Böttcher et al. (2008) suggested that the slowly variable, hard TeV emission of 1ES 1101-232 might be created via Compton up-scattering of CMB photons by shock-accelerated electrons in an extended jet (kiloparsec scale). X-ray emissions from the extended jets of blazars have been detected (e.g., Tavecchio et al. (2007); Sambruna et al. (2008); Massaro et al. (2011)). These evidences imply the presence of high energy electrons in their extended jets. In such an extended jet, the CMB photons would be dominant soft photons for IC process (e.g., Tavecchio et al. (2000)), and the emission of Compton up-scattering of the EBL photons off relativistic electrons may be also important at TeV band (Georganopoulos et al. 2008), due to the Doppler effect. Moreover, recent studies indicated that electrons in the large-scale jets of AGNs may be accelerated to high energies by stochastic acceleration (e.g., Fan et al. (2008); O'Sullivan et al. (2009)). The possible TeV emissions from the extended jets of some radio galaxies have been explored (e.g., Hardcastle & Croston (2011)). In the AGN unified scheme (Urry & Padovani 1995), it is natural and worthwhile to wonder whether the kind of non-variable TeV emissions of some blazars can be produced at least in part in their extended jets.

In this paper, we study possible TeV emission from the extended jet of a blazar. We assume that multi-band emission from a non-variable TeV blazar includes two components: one is from the inner jet and the other is from the extended jet. In this model, the emission from the inner jet is produced in a conventional SSC model; and the emission from the extended jet is produced in a self-consistent SSC+IC/CMB/EBL model under the stochastic acceleration scenario. We apply the model to explain the non-variable hard TeV emission of 1ES 1101-232. The cosmological parameters $(H_0, \Omega_m, \Omega_\Lambda) = (70\ \mathrm{km\ s^{-1}\ Mpc^{-1}}, 0.3, 0.7)$ are used throughout this paper.

2 THE MODEL

As mentioned above, we assume that the emission from a non-variable TeV blazar is produced at both inner and extended jet. In this model, non-thermal photons are produced by both the synchrotron radiation and IC scattering of relativistic electrons in a spherical blob which is moving relativistically at a small angle to our line of sight, and the observed radiation is strongly boosted by a relativistic Doppler factor $\delta_{\rm D}$. We give the specific descriptions of this model below.

2.1 The conventional SSC model in the inner jet

We use the conventional SSC model to produce the emission from the inner jet. Here we assume a broken power-law electrons energy distribution and use the relativistic electron distribution given by Dermer et al. (2009), i.e.,

$$
\begin{aligned}
N'_{\rm e}(\gamma') = K'_{\rm e} H(\gamma'; \gamma'_{\rm min}, \gamma'_{\rm max})\{\gamma'^{-p_1} \exp(-\gamma'/\gamma'_{\rm b}) \\
\times H[(p_2-p_1)\gamma'_{\rm b} - \gamma'] + [(p_2-p_1)\gamma'_{\rm b}]^{p_2-p_1}\gamma'^{-p_2} \\
\times \exp(p_1-p_2) H[\gamma' - (p_2-p_1)\gamma'_{\rm b}]\}, \qquad (1)
\end{aligned}
$$

where $K'_{\rm e}$ is the normalization factor, in unit of $\mathrm{cm^{-3}}$. $H(x; x_1, x_2)$ is the Heaviside function: $H(x; x_1, x_2) = 1$ for $x_1 \leqslant x \leqslant x_2$ and $H(x; x_1, x_2) = 0$ everywhere else; as well as $H(x) = 0$ for $x < 0$ and $H(x) = 1$ for $x \geqslant 0$. The minimum and maximum energies of electrons in the blob are $\gamma'_{\rm min}$ and $\gamma'_{\rm max}$, respectively. The spectrum is smoothly connected with indices p_1 and p_2 below and above the electron's break energy $\gamma'_{\rm b}$. Note that here and throughout the paper, unprimed quantities refer to the distant observer's frame on the Earth and primed ones refer to the co-moving frame.

Then, the synchrotron flux is calculated as (Finke et al. 2008)

$$
\nu F_\nu^{\rm syn} = \frac{\sqrt{3}\delta_{\rm D}^4 \epsilon' e^3 B'}{4\pi h d_{\rm L}^2} \int_0^\infty d\gamma' N'_e(\gamma')(4\pi R'^3_{\rm b}/3) R(x) \ , \qquad (2)
$$

where e is the electron charge, B' is the magnetic field strength, $R'_{\rm b}$ is blob's radius, h is the Planck constant, and $d_{\rm L}$ is the distance to the source with a redshift z. Here $m_{\rm e}c^2\epsilon' = h\nu(1+z)/\delta_{\rm D}$ is synchrotron photons energy in the co-moving frame, where $m_{\rm e}$ is the rest mass of electron and c is the speed of light. Here we use an approximation for $R(x)$ given by Finke et al. (2008). The synchrotron spectral energy density is

$$
u'_{\rm syn}(\epsilon') = \frac{R'_{\rm b}}{c}\frac{\sqrt{3}e^3 B'}{h} \int_0^\infty d\gamma' N'_e(\gamma') R(x) \ . \qquad (3)
$$

The SSC flux νF_ν is given by Finke et al. (2008)

$$
\nu F_\nu^{\rm SSC} = \frac{3}{4} c\sigma_{\rm T}\epsilon'^2_s \frac{\delta_{\rm D}^4}{4\pi d_{\rm L}^2} \int_0^\infty d\epsilon' \frac{u'_{\rm syn}(\epsilon')}{\epsilon'^2}
$$

$$
\times \int_{\gamma'_{\rm min}}^{\gamma'_{\rm max}} d\gamma' \ \frac{N'_e(\gamma')(4\pi R'^3_{\rm b}/3)}{\gamma'^2} F_{\rm C}(q', \Gamma'_{\rm e}) \ , \qquad (4)
$$

where $\sigma_{\rm T}$ is the Thomson cross section, $m_e c^2 \epsilon'_s = h\nu(1+z)/\delta_{\rm D}$ is the energy of IC scattered photons in the co-moving frame, $F_{\rm C}(q', \Gamma'_{\rm e}) = 2q'{\rm ln}q' + (1+2q')(1-q') + \frac{q'^2\Gamma'^2_{\rm e}}{2(1+q'\Gamma'_{\rm e})}(1-q')$, $q' = \frac{\epsilon'/\gamma'}{\Gamma'_{\rm e}(1-\epsilon'/\gamma')}$, $\Gamma'_{\rm e} = 4\epsilon'\gamma'$, and $\frac{1}{4\gamma'^2} \leqslant q' \leqslant 1$.

2.2 The self-consistent SSC+IC/CMB/EBL model in the extended jet under the stochastic acceleration scenario

The self-consistent SSC+IC/CMB/EBL model including a acceleration process in the stochastic acceleration scenario is used to create the emission from the extended jet. A physical self-consistent description of stochastic acceleration in a time evolution scenario can be achieved through a kinetic equation, and the kinetic equation is given as (Katarzyński et al. (2006b); also see Tramacere et al. (2011) and Weidinger et al. (2010))

$$\frac{\partial N'(\gamma',t)}{\partial t} = \frac{\partial}{\partial\gamma'}\left[\left\{C'(\gamma',t) - A'(\gamma',t)\right\}N'(\gamma',t)\right]$$
$$+\frac{\partial}{\partial\gamma'}\left[D'(\gamma',t)\frac{\partial N'(\gamma',t)}{\partial\gamma'}\right] - E'(\gamma',t) + Q'(\gamma',t)\ , \qquad (5)$$

where $D'(\gamma',t)$ is the momentum diffusion coefficient and $A'(\gamma',t) = (2/\gamma')D'(\gamma',t)$ is the average energy change term resulting from the momentum-diffusion process. In this work we assume that the acceleration timescale $t_{\rm acc}$ and escape timescale $t_{\rm esc}$ are both independent of electron energy, which is the case of the hard sphere approximation. Hence, $D'(\gamma') = (1/2t_{\rm acc})\gamma'^2$, $A'(\gamma') = \gamma'/t_{\rm acc}$ and the escape term $E'(\gamma') = N'(\gamma',t)/t_{\rm esc}$. $Q'(\gamma',t)$ is the injection term. $C'(\gamma',t)$ is the total cooling rate. In addition to the synchrotron cooing rate $(\frac{d\gamma'}{dt})_{\rm syn}$ and SSC cooling rate $(\frac{d\gamma'}{dt})_{\rm SSC}$, we consider the IC/CMB cooling rate $(\frac{d\gamma'}{dt})_{\rm IC/CMB}$ and IC/EBL cooling rate $(\frac{d\gamma'}{dt})_{\rm IC/EBL}$. Therefore, $C'(\gamma',t) = (\frac{d\gamma'}{dt})_{\rm syn} + (\frac{d\gamma'}{dt})_{\rm SSC} + (\frac{d\gamma'}{dt})_{\rm IC/CMB} + (\frac{d\gamma'}{dt})_{\rm IC/EBL}$. For synchrotron cooling, $(\frac{d\gamma'}{dt})_{\rm syn} = \frac{4\sigma_{\rm T}c}{3m_{\rm e}c^2}U'_{\rm B}\gamma^2$, where $U'_{\rm B} = \frac{B'^2}{8\pi}$ is the magnetic field energy density. The SSC cooling rate using the full KN cross section (e.g., Jones (1968); Böttcher et al. (1997); Finke et al. (2008)) is

$$(\frac{d\gamma'}{dt})_{\rm SSC} = \frac{3\sigma_{\rm T}}{8m_{\rm e}c}\int_0^\infty d\epsilon'\frac{u'_{\rm syn}(\epsilon')}{\epsilon'^2}\ G(\gamma'\epsilon') \qquad (6)$$

where $G(E) = \frac{8}{3}E\frac{1+5E}{(1+4E)^2} - \frac{4E}{1+4E}\left(\frac{2}{3}+\frac{1}{2E}+\frac{1}{8E^2}\right) + \ln(1+4E)\left(1+\frac{3}{E}+\frac{3}{4}\frac{1}{E^2}+\frac{\ln[1+4E]}{2E}-\frac{\ln[4E]}{E}\right) - \frac{5}{2}\frac{1}{E} + \frac{1}{E}\sum_{n=1}^{\infty}\frac{(1+4E)^{-n}}{n^2} - \frac{\pi^2}{6E} - 2$, and $u'_{\rm syn}(\epsilon')$ is given by equation (3). We calculate the IC/CMB and IC/EBL cooling rates using the method given by Moderski et al. (2005), which fully takes into account KN effects,

$$(\frac{d\gamma'}{dt})_{\rm IC/CMB/EBL} = \frac{4\sigma_{\rm T}c}{3m_{\rm e}c^2}\gamma'^2F_{\rm KN}\ , \qquad (7)$$

where $F_{\rm KN} = \int_{\epsilon'_{\rm min}}^{\epsilon'_{\rm max}} f_{\rm KN}(4\gamma'\epsilon')u'_{\rm CMB/EBL}(\epsilon')d\epsilon'$. $f_{\rm KN}(x) \simeq \frac{9}{2x^2}({\rm ln}x - 11/6)$ for $x \gg 1$. $f_{\rm KN}(x)$ can be approximated by $f_{\rm KN}(x) \simeq 1/(1+x)^{1.5}$ for $x \lesssim 10^4$. For the case of the CMB radiation in the stationary frame of the host galaxy, $u_{\rm CMB}(\epsilon) = \frac{8\pi m_{\rm e}c^2(m_{\rm e}^3c^3)}{h^3}\frac{\epsilon^3}{\exp(\epsilon/\Theta)-1}$, where $\Theta = \kappa_{\rm B}T/m_{\rm e}c^2$ is the dimensionless temperature of the blackbody radiation field, $T = 2.72(1+z)$ K and $\kappa_{\rm B}$ is the Boltzmann constant. We use the spectral EBL energy density expected in Finke et al. (2010). The spectral energy densities in the co-moving frame transform as $u'(\epsilon') = \delta_{\rm D}u(\epsilon'/\delta_{\rm D})$ (e.g.,Ghisellini & Tavecchio (2009)).

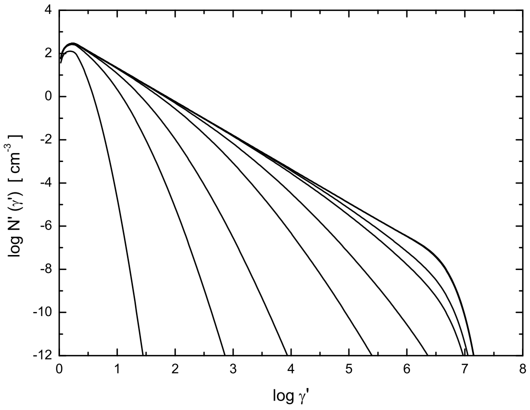

Figure 1. The reproduced electron spectra in Fig. 4 of Katarzyński et al. (2006b) by using our code.

To obtain the self-consistent relativistic electron energy distribution, we must solve equation (5) numerically. In the numerical calculations, we adopt the numerical method given by Park & Petrosian (1996), which is firstly proposed by Chang & Copper (1970). The method is a finite difference scheme, which uses the centered difference of the diffusive term, and a weighted difference for the advective term. We have carefully tested our code by running it with parameters identical to those used for Fig. 4 of Katarzyński et al. (2006b), only considering the synchrotron and SSC radiative cooling. We find good agreement with their results. The reproduced electron spectra in Fig. 4 of Katarzyński et al. (2006b) using our code are shown in our Fig. 1.

After obtaining the relativistic electron energy distribution, we can calculate the synchrotron-SSC flux and IC/CMB/EBL flux from the extended jet by using equation (2) and equation (4) with the corresponding electron spectrum and energy densities of soft photons field.

High energy emission from both the inner and extended jet would be modified by a factor of $\exp(-\tau)$ due to the absorption of EBL. In this paper, we use the optical depth τ expected in Finke et al. (2010). This EBL model is a low level one, which is consistent with the widely used one (e.g., Franceschini et al. (2008)) and the newly proposed one (e.g., Domínguez et al. (2011)).

3 APPLICATION TO 1ES 1101-232

1ES 1101-232 resides in an elliptical host galaxy (e.g., Remillard et al. (1989)). An extended jet structure at a few kiloparsec distance from the core is revealed by the radio observations (Laurent-Muehleisen et al. (1993)). The TeV observations of 1ES 1101-232 were performed by the H.E.S.S. Cherenkov telescopes in April and June 2004, and in March 2005. Simultaneous observations were carried out with H.E.S.S., X-ray measurements with RXTE, and optical measurements with the ROTSE 3c robotic telescope in March 2005, following the detection of a weak signal in

Table 1. The modeling parameters for the inner and extended jets.

inner jet	B' (G)	$\gamma'_{\rm min}$	$\gamma'_{\rm max}$	$\gamma'_{\rm b}$	$\delta_{\rm D}$	$K'_{\rm e}$ ($\rm cm^{-3}$)	p_1	p_2	$R'_{\rm b}$ (cm)
	0.1	1.0	6.0×10^5	2.0×10^5	24.7	19.8	2.0	4.0	7.5×10^{16}

extended jet	B' (μG)	Q' ($\rm cm^{-3}\ s^{-1}$)	$R'_{\rm b}$ (cm)	$t_{\rm esc}$ (s)	$t_{\rm acc}/t_{\rm esc}$	$\delta_{\rm D}$	$U'_{\rm e}/U'_{\rm B}$
highly beamed	23.0	8.0×10^{-20}	5.0×10^{20}	$R'_{\rm b}/c$	0.86	15	1.0
moderately beamed	58.5	5.0×10^{-19}	5.0×10^{20}	$R'_{\rm b}/c$	0.86	10	1.0
mildly beamed	29.3	1.0×10^{-17}	5.0×10^{20}	$R'_{\rm b}/c$	0.78	5	112.3

Table 2. The radiative ($P_{\rm r}$), Poynting flux ($P_{\rm B}$), kinetic ($P_{\rm e}$ and $P_{\rm p}$), and injection ($L_{\rm inj}$) powers for the inner and extended jets.

inner jet	$P_{\rm r}$ ($\rm erg\ s^{-1}$)	$P_{\rm B}$ ($\rm erg\ s^{-1}$)	$P_{\rm e}$ ($\rm erg\ s^{-1}$)	$P_{\rm p}$ ($\rm erg\ s^{-1}$)
	4.1×10^{43}	1.3×10^{44}	5.4×10^{43}	9.2×10^{45}

extended jet	$P_{\rm r}$ ($\rm erg\ s^{-1}$)	$P_{\rm B}$ ($\rm erg\ s^{-1}$)	$P_{\rm e}$ ($\rm erg\ s^{-1}$)	$P_{\rm p}$ ($\rm erg\ s^{-1}$)	$L_{\rm inj}$ ($\rm erg\ s^{-1}$)
highly beamed	2.5×10^{43}	1.1×10^{44}	1.1×10^{44}	1.5×10^{43}	5.2×10^{40}
moderately beamed	1.2×10^{44}	3.2×10^{44}	3.2×10^{44}	4.1×10^{43}	1.4×10^{41}
mildly beamed	2.4×10^{44}	2.0×10^{43}	2.3×10^{45}	2.0×10^{44}	7.2×10^{41}

the 2004 H.E.S.S. observations (Aharonian et al. 2007c). No TeV variability was found in these observations, and a moderate flux changes were observed with RXTE in March 2005 (Aharonian et al. 2007c). No very significant signal from 1ES 1101-232 is detected by *Fermi*-LAT in its first year scientific operation (Abdo et al. 2010), and only the flux upper limits derived from the first year *Fermi*-LAT observations are available (e.g., Neronov & Vovk (2010); Costamante (2011)). The two years scientific operation of *Fermi*-LAT reports a significant detection of 1ES 1101-232 at a significance 5.2σ with the photon spectral index $\Gamma = 1.80 \pm 0.31$ (Ackermann et al. 2011). More significant signals ($\sigma \sim 10$) from 1ES 1101-232 have been detected in *Fermi*-LAT's 3.5 years observations (Finke et al. 2012). We will use *Fermi*-LAT 3.5 years average spectrum. Since the detections made by H.E.S.S. in 2004 are not significant, we select the simultaneous multi-band data derived in the observations in March 2005 in this paper.

The variability at optical and X-ray frequencies of 1ES 1101-232 have been detected (e.g., Remillard et al. (1989); Romero et al. (1999); Wolter et al. (2000)). Moreover, the IC/CMB process having a radiative cooling timescale $\sim 10^3$ years (Böttcher et al. (2008)), such long cooling timescale indicates that IC/CMB emission, as well as the synchrotron emission associated with the same high energy electrons and emission region, will be slowly variable. In addition, the very large size of the emission region in the extended jet (e.g., Tavecchio et al. (2007); Fan et al. (2008)) also indicates that emission from such a region should be slowly variable. We therefore argue that the moderately variable optical-X-ray radiation of 1ES 1101-232 should be dominated by the emissions originating in a compact region in the inner jet.

As discussed above, we use the conventional SSC model in the inner jet to produce the optical-X-ray emission. The self-consistent SSC+IC/CMB/EBL model is used to create the TeV emission from the extended jet. In the extended jet, we assume that electrons with energy $\gamma'_{\rm inj} \approx 27$ are continuously injected into a blob with a constant injection rate Q'. The minimum and maximum energies of electrons in this blob are set as $\gamma'_{\rm min} = 1.0$ and $\gamma'_{\rm max} = 10^7$.

The Doppler effect is crucial for the IC/CMB/EBL emission because it can affect the CMB energy density and the CMB photons energy in the co-moving frame, and inversely it affects the relativistic electrons energy density required to produce the TeV emission. Unfortunately, Doppler factor is poorly constrained. It is possible that the jets of blazars remain highly relativistic at kiloparsec scales (e.g., Atoyan & Dermer (2004); Jorstad & Marscher (2004)). However, recent very long baseline interferometry (VLBI) observations indicate that the bulk Lorentz factors in the parsec-scale radio jets of TeV HBLs are fairly low, $\Gamma < 5$ (e.g.,Piner et al. (2008, 2010)). Because of the importance of Doppler effect, we assume three values of Doppler factor for the TeV emission region in the extended jet, which are $\delta_{\rm D} = 15, 10, 5$ corresponding to the highly beamed, moderately beamed and mildly beamed cases respectively, to reproduce the TeV emission of 1ES 1101-232. In the following, we show the results of reproducing SED.

The case of highly beamed extended jet with $\delta_{\rm D} = 15$: the results are shown in Fig. 2. It can be seen that when $t > 9\ t_{\rm acc}$, the electron spectrum produced by the stochastic acceleration tends to be steady. This distribution in steady-state develops a rising low-energy power-law tail (left side of $\gamma'_{\rm inj}$ in upper panel of Fig. 2) with the theoretic spectral index $n \simeq -2 - \frac{t_{\rm acc}}{2t_{\rm esc}}$ (the acceleration theory predicts $n \simeq -2.43$, and our numerical calculations give $n \approx -2.49$), but at high energies it presents a power-law spectrum with an exponential cut-off (right side of $\gamma'_{\rm inj}$ in upper panel of Fig. 2). The spectral index of power-law distribution formed in the stochastic acceleration scenario at $\gamma' > \gamma'_{\rm inj}$ is $n \simeq 1 + \frac{t_{\rm acc}}{2t_{\rm esc}}$ (the acceleration theory predicts $n \simeq 1.43$, and our numerical calculations give $n \approx 1.49$), which differs from the spectral index $n \simeq 1 + \frac{t_{\rm acc}}{t_{\rm esc}}$ that obtained from the basic shock acceleration (e.g., Kirk et al. (1998); Katarzyński et al. (2006b)). The cut-off energy can be obtained when the cooling time scale $t_{\rm cool}$ satisfies the condition $t_{\rm cool}(\gamma_{\rm c}') = t_{\rm acc}$. We adopt this steady-state electron spectrum to produce the TeV emission from the extended jet. As shown in lower panel of Fig. 2, a good representation of SED can be achieved. The synchrotron emission from the inner jet contributes to the optical-X-ray emission of 1ES 1101-232. At GeV band, SSC emission from the inner jet is dominant. The parameters we used are appropriate for the emission region in the inner jet with the ratio between the relativistic electrons energy density and the magnetic field energy density, $U_{\rm e}'/U_{\rm B}' \approx 0.4$. The parameters are listed in Table 1. The IC/CMB emission from the extended jet dominates the TeV emission, while IC/EBL emission as well as the SSC emission from the extended jet are negligible in this case. Our results indicate that the intrinsic TeV flux peak is located at $\sim$ 4 TeV, and the intrinsic TeV spectral index is $\Gamma_{\rm int} \sim 1.5$, which are consistent with that inferred by Aharonian et al. (2007c). As required, the injected power ($L_{\rm inj} = \frac{4}{3}\pi R_{\rm b}'^3 \frac{\delta_{\rm D}^2}{4} Q' \gamma_{\rm inj}' \approx 5.2 \times 10^{40}$ erg s^{-1} (Weidinger 2011)) in the stationary frame of the host galaxy for the extended jet (see Table 2) exceeds the observed radio power of the extended radio structure at 1.5 GHz, $L_{1.5}^{\rm ext} \approx 3.8 \times 10^{40}$ erg s^{-1} (Laurent-Muehleisen et al. 1993). Because of the highly relativistic extended jet, the required energy density of relativistic electrons is small, $U_{\rm e}' \approx 2.1 \times 10^{-11}$ erg cm^{-3}. The parameters we adopted for the extended jet can achieve the equipartition condition between the relativistic electrons and the magnetic field ($U_{\rm e}'/U_{\rm B}' \approx 1.0$), and the synchrotron emission from the extended jet is about one order of magnitude below the emission from the inner jet.

The case of moderately beamed extended jet with $\delta_{\rm D} = 10$: the results are presented in Fig. 3. In this case, we only present the electron spectrum in the steady state, which is used to reproduce the TeV emission from the extended jet, since the evolution of this electron spectrum is the same as that in the former case. The emissions from the inner jet are the same as that in the former case, and TeV emission is also dominated by IC/CMB emission. In this case, the required energy density of relativistic electrons becomes larger, $U_{\rm e}' \approx 1.4 \times 10^{-10}$ erg cm^{-3}. In order to achieve the equipartition with $U_{\rm e}'/U_{\rm B}' \approx 1.0$, a larger magnetic field strength ($U_{\rm B}' \sim 2U_{\rm CMB}'$) is needed, which causes the significant synchrotron emission from the extended jet. If a magnetic field in quasi-equipartition with the relativistic electrons with $U_{\rm e}'/U_{\rm B}' \sim 2.0$ is used, the contribution of synchrotron emission from the extended jet will become slight to the optical-X-ray emission of 1ES 1101-232.

The case of mildly beamed extended jet with $\delta_{\rm D} = 5$: we show the results in Fig. 4. The emissions from the inner jet are still unchanged. In this case, for reproducing the TeV emission well, a high energy density of relativistic electrons in the extended jet is needed, $U_{\rm e}' \approx 3.8 \times 10^{-9}$ erg cm^{-3}. Even a large magnetic field strength is used ($U_{\rm B}' \sim 2U_{\rm CMB}'$), the parameters with $U_{\rm e}'/U_{\rm B}' \approx 112.3$ still largely deviate from the equipartition.

We now can estimate the powers in the forms of radiation ($P_{\rm r}$), Poynting flux ($P_{\rm B}$), relativistic electrons ($P_{\rm e}$) and

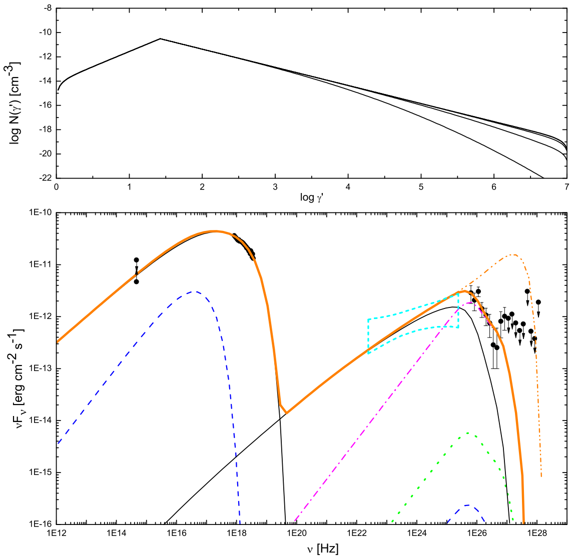

Figure 2. The case of highly beamed extended jet with $\delta_{\rm D} = 15$. Upper panel: the evolution of the electron spectrum in the extended jet. From left to right: t= (3, 5, 7, 9, 13) $t_{\rm acc}$. Lower panel: SED of 1ES 1101-232. The filled circles are the simultaneous optical - X-ray - TeV data taken from Aharonian et al. (2007c). The area surrounded by short-dashed line is the *Fermi*-LAT 3.5 years average spectrum integrated over August 2008 to February 2012 (Finke et al. 2012). The curves represent synchrotron-SSC emission from the inner jet (thin solid line), synchrotron-SSC emission from the extended jet (dashed line), IC/EBL emission from the extended jet (dotted line) and IC/CMB emission from the extended jet (dot-dashed line). The thick solid line is the total emission from the inner and extended jet with absorption of EBL and the double-dot-dashed line is the intrinsic total spectrum without absorption of EBL.

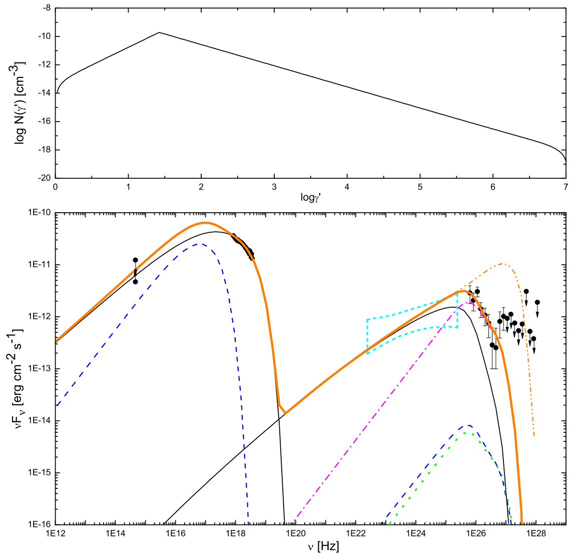

Figure 3. The case of moderately beamed extended jet with $\delta_{\rm D} = 10$. Upper panel: the electron spectrum in steady state. Lower panel: SED of 1ES 1101-232. The symbols and curves are the same as that in Fig. 2.

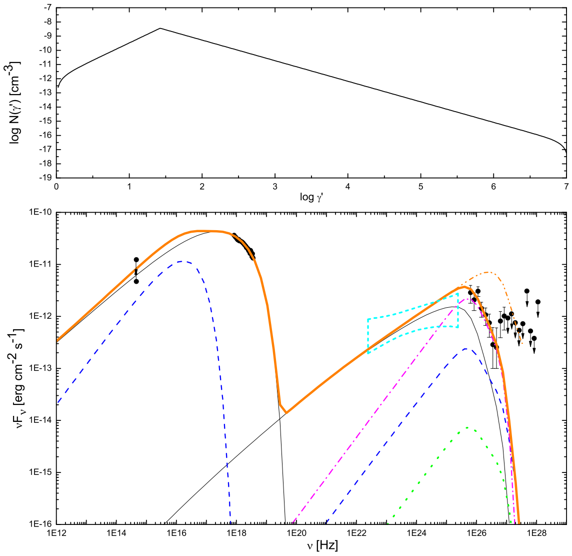

Figure 4. The case of mildly beamed extended jet with $\delta_{\rm D} = 5$. Upper panel: the electron spectrum in steady state. Lower panel: SED of 1ES 1101-232. The symbols and curves are the same as that in Fig. 2.

protons ($P_{\rm p}$) for the inner and extended jet, respectively, which are all in the stationary frame of the host galaxy. All the powers are calculated as (Celotti & Fabian 1993; Celotti & Ghisellini 2008)

$$P_{\rm i} = \pi R_{\rm b}^{\prime 2} \Gamma^2 U_{\rm i}^{\prime} c \ , \tag{8}$$

where $U_{\rm i}^{\prime}$ (i=r, e, B, p) are the energy densities associated with the radiation $U_{\rm r}^{\prime}$, the emitting electrons $U_{\rm e}^{\prime}$, magnetic field $U_{\rm B}^{\prime}$ and protons $U_{\rm p}^{\prime}$ in the comoving frame. We calculate $U_{\rm p}^{\prime}$ by assuming one proton per emitting electron, then $U_{\rm p}^{\prime} = U_{\rm e}^{\prime}(m_{\rm p}/m_{\rm e})/\langle\gamma^{\prime}\rangle$ (Celotti & Ghisellini 2008), where $\langle\gamma^{\prime}\rangle$ is the average energy of relativistic electrons. Here, we take the bulk Lorentz factor $\Gamma = \delta_{\rm D}$. The power carried in the form of the produced radiation can be rewritten as by using $U_{\rm r}^{\prime} = L^{\prime}/(\pi R_{\rm b}^{\prime 2} c)$ (Celotti & Ghisellini 2008)

$$P = L^{\prime}\Gamma^2 \approx L\frac{\Gamma^2}{\delta_{\rm D}^4} \ , \tag{9}$$

where L is total no-thermal luminosity.

Our predicted powers are listed in Table 2. For the inner jet, we have that $P_{\rm r} \sim P_{\rm e} \leqslant P_{\rm B}$. This follows the fact that the synchrotron luminosity from the inner jet is larger than the γ-ray one. For the extended jets with $\delta_{\rm D} = 10, 15$, we have that $P_{\rm r} \sim P_{\rm e} \sim P_{\rm B}$. Since $P_{\rm r} \sim P_{\rm e}$, relativistic electrons cannot be the primary energy carriers in the jet (Celotti & Ghisellini 2008). Under the assumption of one proton per emitting electron, our results indicate that a substantial fraction of the total jet power in the inner jet is carried by protons. However, it can be seen that in the extended jet, the jet power in protons is far smaller than the one in emitting electrons, with $P_{\rm p}/P_{\rm e} \sim 0.1$, which contradicts the scenario that a sizeable fraction of jet power is carried out to large distances by the protons content of the jet. Moreover, Poynting flux in the inner jet is comparable with the ones in the extended jets for the cases of $\delta_{\rm D} = 10, 15$. Therefore, relativistic leptons as well as Poynting flux also cannot be the primary energy carriers. It is likely that for the case of 1ES 1101-232 the cold electron positron pairs are the primary energy carriers in the jet (e.g., Celotti & Ghisellini (2008)).

As mentioned in introduction, Böttcher et al. (2008) have modeled the TeV emission from 1ES 1101-232 in the frame of Compton up-scattering of CMB photons by shock-accelerated electrons in an extended jet with $\delta_{\rm D} = 15$. It is worthwhile to compare their results with ours. For the extended jet with $\delta_{\rm D} = 15$, the injected power in our model is $L_{\rm inj} = 5.2 \times 10^{40}$ erg s^{-1} (see Table 2), which is about 1/3 of that given by Böttcher et al. (2008). The electrons distribution index used by Böttcher et al. (2008) is $n = 1.5$, which is almost the same as that we obtained ($n \approx 1.49$). However, in the framework of shock acceleration, such a small electrons distribution index can only result from the extreme condition (Stecker et al. 2007), while in the stochastic acceleration model, such a small one can be naturally obtained assuming $t_{\rm acc} \sim t_{\rm esc}$. In order to achieve the equipartition, a larger value ($\sim$ 23 μG and $U_{\rm B}^{\prime} \approx 0.1 U_{\rm CMB}^{\prime}$, where $U_{\rm CMB}^{\prime} = 4.02 \times 10^{-13}(1+z)^4\delta_{\rm D}^2$ erg cm^{-3}) of magnetic field strength is required in our model compared to that ($\sim$ 10 μG) used in Böttcher et al. (2008), which causes the larger synchrotron emission from extended jet than that derived in Böttcher et al. (2008). For the inner jet, we assumed a broken power-paw electrons distribution to create the non-thermal emission. It can be found that the values of $B^{\prime}$,$R_{\rm b}^{\prime}$, $\delta_{\rm D}$ and $\gamma_{\rm max}^{\prime}$ used in our model are very close to those used by Böttcher et al. (2008). However, the value of $\gamma_{\rm min}^{\prime}$ can be as low as one in our inner jet model ($\gamma_{\rm min}^{\prime} \sim 10^5$ in Böttcher et al. (2008)).

4 DISCUSSION AND CONCLUSION

Recently, some studies indicate that particles in the large-scale jets of radio galaxies would be accelerated to high energies through the stochastic acceleration (e.g., Hardcastle et al. (2008); O'Sullivan et al. (2009)). Actually, the stochastic acceleration has been applied to explain emissions from the inner jets of blazars (e.g., Wang (2002); Katarzyński et al. (2006b); Tramacere et al. (2011)). It is likely that several acceleration mechanisms may be acting in parallel in the jets of AGNs (e.g., Rieger et al. (2007)). Because of the detections of X-ray and GeV emissions from the extended jets of blazars and radio galaxies (e.g., Abdo et al. (2010); Massaro et al. (2011)), we think it is worthwhile to investigate whether TeV emission could be created in the extended jet of a blazar. In this paper, we assume that electrons in the extended jet of 1ES 1101-232 can be accelerated to high energies by stochastic acceleration, therefore TeV emission may be produced via Compton up-scattering of CMB and EBL photons by these electrons. The traditional emission from the inner jet should also be taken into account. For simplicity, we use the conventional SSC model to produce this emission from the inner jet. It can be seen that our model can well reproduce the SED of 1ES 1101-232, and its hard TeV emission is dominated by the IC/CMB component from the extended jet. Since our model requires the extent of the emission region in the extended jet to be kiloparsec, the behavior of substantial TeV variability is forbidden. The emissions from a compact region in the inner jet make dominant contribution to the emission of 1ES 1101-

232 at optical- X-ray and GeV band. Therefore, the variabilities on time-scales of days at optical - X-ray and GeV band are allowed. If it is determined that the extended jet is another TeV emission region, this fact will provide stronger constraints on the physics properties of emission region in the inner jet. However, it should be kept in mind that this model is only applicable for the TeV blazars that show no TeV variability (e.g., 1ES 1101-232, 1ES 0229+200 and 1ES 0347-121).

We assumed three characteristic values of Doppler factor for the TeV emission region in the extended jet. We can well reproduce the TeV emission of 1ES 1101-232 using each one of them. Furthermore, for a moderate or a large value of Doppler factor ($\delta_{\rm D} \sim 10, 15$), the physical parameters in the TeV emitting region in the extended jet are consistent with the equipartition (or quasi-equipartition). In contrast, for a small value of $\delta_{\rm D} \sim 5$, the parameters largely depart from the equipartition with $U'_{\rm e}/U'_{\rm B} \gg 1$. Piner et al. (2010) suggested that the bulk Lorentz factors in the TeV emission region and radio emission region of TeV blazar would be different. Therefore, we conclude, from our results, that the TeV emitting region in the extended jet of 1ES 1101-232 should be moderately or highly beamed.

ACKNOWLEDGMENTS

We thank the anonymous referee for his/her very constructive comments. This work is partially supported by a 973 Program (2009CB824800) and Yunnan Province under a grant 2009 OC.

REFERENCES

Abdo, A., A., et al., 2010, Sci, 328, 725
Abdo, A., A., et al., 2010, ApJ, 715, 429
Ackermann, M., et al., 2011, ApJ, 743, 171
Aharonian, F., et al. 2006, Nature, 440, 1018
Aharonian, F., et al., 2007a, A&A, 475, L9
Aharonian, F., et al., 2007b, A&A, 473, L25
Aharonian, F., et al., 2007c, A&A, 470, 475
Aharonian, F. A., Khangulyan, D., & Costamante, L. 2008, MNRAS, 387, 1206
Atoyan, A., & Dermer, C. D. 2004, ApJ, 613, 151
Böttcher, M., Mause, H., & Schlickeiser, R. 1997, A&A, 324, 395
Böttcher, M., Dermer, C. D., & Finke, J. D., 2008, ApJ, 679, L9
Böttcher, M. 2007, Ap&SS, 309, 95
Celotti, A., & Fabian, A. C. 1993, MNRAS, 264, 228
Celotti, A., & Ghisellini, G. 2008, MNRAS, 385, 283
Costamante, L. 2011 Fermi Symposium, Roma.
Chang, J. S., & Copper, G. 1970, J. Comput. Phys., 6, 1
Domínguez, A. et al., 2011, MNRAS, 410, 2556
Dermer, C. D., & Schlickeiser, R. 1993, ApJ, 416, 458
Dermer, C. D., Finke, J. D., Krug, H., & Böttcher, M. 2009, ApJ, 692, 32
Essey, W., Kalashev, O., Kusenko, A., & Beacom, J. F. 2011, ApJ, 731, 51
Fan, Z. H., Liu, S. M., Wang, J. M., Fryer, C. L., & Li, H. 2008, ApJ, 673, L139
Finke, J. D., Dermer, C. D., & Böttcher, M. 2008, ApJ, 686, 181
Finke, J. D., Razzaque, S., & Dermer, C. D. 2010, ApJ, 712, 238
Finke, J. D., Georganopoulos, M., & Reyes, L. for the Fermi-LAT Collaboration, "Constraints on the Extragalactic Background Light from Gamma-Ray Observations", SnowTIGER 2012, Snowbird, Utah, March 2012
Franceschini, A., Rodighiero, G., & Vaccari, M. 2008, A&A, 487, 837
Georganopoulos, M. et al., 2008, ApJ, 686, L5
Ghisellini, G. & Tavecchio, F., 2009, MNRAS, 397, 985
Hardcastle, M. J., Cheung C. C., Feain I. J., Stawarz L., 2008, MNRAS, 393, 1041
Hardcastle, M. J., & Croston, J. H., 2011, MNRAS, 415, 133
Jorstad, S. G., & Marscher, A. P., 2004, ApJ, 614, 615
Jones, F. C. 1968, Phys. Rev., 167, 1159
Katarzyński, K., Ghisellini, G., Tavecchio, F., Gracia, J., & Maraschi, L. 2006a, MNRAS, 368, L52
Katarzyński, K., Ghisellini, G., Mastichiadis, A., Tavecchio, F., & Maraschi, L. 2006b, A&A, 453, 47
Kirk, J. G., Rieger, F. M., & Mastichiadis, A. 1998, A&A, 333, 452
Laurent-Muehleisen, S. A., Kollgaard, R. I., Moellenbrock, G. A., & Feigelson, E. D. 1993, AJ, 106, 875
Lefa, E., Rieger, F. M., & Aharonian, F. A. 2011a, ApJ, 740, 64
Lefa, E., Aharonian, F., & Rieger, F. M. 2011b, ApJ, 743, L19
Mannheim, K., 1993, A&A, 269, 67
Maraschi, L., Ghisellini, G., & Celotti, A. 1992, ApJL, 397, L5
Massaro, F., Harris, D. E., & Cheung, C. C., 2011, ApJS, 197, 24
Moderski, R., Sikora, M., Coppi, P. S., & Aharonian, F. 2005, MNRAS, 363, 954
Mücke, A., Protheroe, R. J., Engel, R. et al. 2003, APh, 18, 593
Neronov, A.,& Vovk, I., 2010, Sci, 328, 73
O'Sullivan, S., Reville, B., & Taylor, A. M. 2009 MNRAS, 400, 248
Park, B. T., & Petrosian, V. 1996, ApJS, 109, 255
Piner, B. G., Pant, N., Edwards, P. G., 2008, ApJ, 678, 64
Piner, B. G., Pant, N., Edwards, P. G., 2010, ApJ, 723, 1150
Rees, M. J. 1967, MNRAS, 137, 429
Remillard, R. A., Tuhoy, I. R., Brissenden, R. J. V., et al. 1989, ApJ, 345, 140
Rieger, F., Bosch-Ramon, V., Duffy, P., 2007, Ap&SS, 309, 119
Romero, G. E., Cellone, S. A., & Combi, J. A. 1999, A&AS, 135, 477
Sambruna, R. M., Donato, D., Cheung, C. C., Tavecchio, F., Maraschi, L. 2008, ApJ, 684, 862
Stecker, F. W., de Jager, O. C., & Salamon, M. H. 1992, ApJ, 390, L49
Stecker, F. W., Baring, M. G., & Summerlin, E. J. 2007, ApJ, 667, L29
Sikora, M., Begelman, M. C., & Rees, M. J. 1994, ApJ, 421, 153
Tavecchio, F., Maraschi, L., Sambruna, R. M., & Urry, C.

M., 2000, ApJ, 544, L23
Tavecchio, F., Maraschi, L., Wolter, A., Cheung, C. C., Sambruna, R. M., Urry, C. M. 2007, ApJ, 662, 900
Tavecchio, F., Ghisellini, G., Ghirlanda, G., Costamante, L., & Franceschini, A. 2009, MNRAS, 399, 59
Tramacere, A., Massaro, E.,& Taylor, A. M. 2011, ApJ, 739, 66
Urry, C. M., & Padovani, P., 1995, PASP, 107, 803
Wang, J. C., 2002, ChJAA, 2, 1
Weidinger, M., Rüger, M., & Spanier, F., 2010, Astrophys. Space Sci. Trans., 6, 1
Weidinger, M., PhD thesis, 2011, University of Wuerzburg
Wolter, A., Tavecchio, F., Caccianiga, A., Ghisellini, G., & Tagliaferri, G., 2000, A&A, 357, 429
Zacharopoulou, O., Khangulyan, D., Aharonian, F., & Costamante, L. 2011, ApJ, 738, 157